DYNAMIC LARGE EDDY SIMULATION: BENEFITS OF HONORING REALIZABILITY

Ghazaleh Ahmadi
ForWind
Carl von Ossietzky University
Küpkersweg 70, 26129 Oldenburg, Germany
ghazaleh.ahmadi@uni-oldenburg.de

Hassan Kassem
Fraunhofer IWES
Fraunhofer Institute for Wind Energy Systems
Küpkersweg 70, 26129 Oldenburg, Germany
hassan.kassam@iwes.fraunhofer.de

Joachim Peinke
ForWind, Fraunhofer IWES
Carl von Ossietzky University
Küpkersweg 70, 26129 Oldenburg, Germany
joachim.peinke@uni-oldenburg.de

Stefan Heinz
Department of Mathematics
University of Wyoming
Ross Hall 214, Laramie, Wyoming, USA
heinz@uwyo.edu

ABSTRACT

The use of stochastic analysis enables a theoretically well based, systematic derivation of a probability density function (PDF)-realizable dynamic LES model. However, this PDF-realizable model is not always stable due to the rare appearances of non-realizable SGS stress values. The stability of dynamic simulations is a difficult challenge specially in complex wall-bounded flow with high Reynolds numbers. Based on the premise that the sub-grid scale (SGS) model contributions is relatively small, many researchers suggested implicit LES (iLES) as a realizable alternative. On the other hand, it has been shown that ensuring the fully realizability of the SGS stress tensor (stress-realizability) solves the potential instability of the dynamic LES. Nevertheless, this approach implies dynamic bounding of the SGS stress in the dynamic LES calculations.

Thorough realizability and stability analyses of PDF- and stress-realizable dynamic LES model (LDMK) are performed for turbulent channel flow and separated hill flow simulations covering a range of Reynolds numbers from very low to high. In addition, stability of dynamic LES of neutral Atmospheric Boundary Layer (ABL) on a flat terrain is investigated with with a Reynolds number Re five orders of magnitude higher than in other simulations. Results show that the stability of ABL computations is ensured by enforcing the newly developed dynamic realizability bounds. The suggested method of stabilization is applicable to other dynamic LES models. Unlike the fully realizable model, iLES is not capable of producing any turbulent viscosity as required for a high Reynolds number flow or coarse grid applied. This limits the applicability of iLES to simple flows with low Reynolds number (it is not applicable to ABL flow simulations).

Introduction

Large Eddy Simulation (LES) (Meneveau & Katz (2000); Germano (2000); Piomelli (1999)) has been empowered due to its ability to resolve the dominant turbulence structures and its relatively lower computational cost compared to Direct Numerical Simulation (DNS) (Spalart *et al.* (1997); Pope (2000); Sagaut (2002)). In the context of LES, dynamic LES is known to be the state-of-the-art solution to overcome the necessity of the empirical wall models to simulate wall-bounded flows (Lilly (1992); Meneveau *et al.* (1996); Ghosal *et al.* (1995); Piomelli & Liu (1995)). Nevertheless, dynamic calculation of the model parameter can cause numerical instabilities (Germano *et al.* (1991)) which tend to become very challenging in simulations with very high Reynolds numbers. The source of the numerical instability is explained by researchers (Lund *et al.* (1993); Mokhtarpoor & Heinz (2017)) but the challenge still stands, specially in the wall-bounded flows with high Reynolds number. According to Mokhtarpoor & Heinz (2017), numerical instability is connected to the unrealizable values of dynamic LES coefficient C_s, the coefficient used to calculate dynamic turbulent viscosity, ν_t. Temporal investigation of C_s shows that the standard deviation tends to increase before the numerical instability happens.

The focus of this research is how to either avoid or overcome the numerical instability challenge for extreme Reynolds number flows. In theory, in order to avoid the numerical instability, one method is ignoring the instability source (ν_t), arguing that the contribution of ν_t is negligible in the effective viscosity and the numerical dissipation is enough to model it. This approach is called implicit LES (iLES)(Drikakis *et al.* (2016); Aspden *et al.* (2008); Deskos *et al.* (2018); Ritos *et al.* (2017)). iLES violates the PDF-realizability of the velocity field by neglecting the contribution of the SGS turbulent structures. Nevertheless, it has no conflict with any realizability constraints in respect to the stress tensor and can be considered stress-realizable. As an alternative approach, honoring the realizability constraints for stress tensor, PDF-realizable dynamic model is suggested in combination with dynamic bounds which ensure stress-realizability (LDMK).

In this work, the assumptions behind iLES are investigated to study the range of validity of it. These studies are performed by examining the dynamic LES of turbulent channel flow in a range of Reynolds numbers from Re_τ=180 to

2000 corresponding to Re_b=2857 to 43478. Also, separated hill flow is studied in a range of Reynolds numbers from Re_b=5500 to 37000. Both simulations are performed on different computational grids to observe the effect of the grid coarsening. iLES and LDMK are investigated in terms of cost and accuracy of simulation of the wall-bounded flow regarding the implications of very high Reynold numbers. In addition, the stability of dynamic LES applied to simulate the neutral Atmospheric Boundary Layer (ABL) flow, is explored. The behavior of the LES coefficient C_s right before the occurrence of the numerical instability and the effect of stress-realizability on the numerical stability are presented at $Re_b = 1.2 \times 10^9$. Considering the very high Reynolds number and the relatively coarse computational grid, iLES is too inaccurate to be used for ABL simulations. Therefore, honoring the realizability regarding the PDF-equation system and stress tensor is left as the only solution to perform and stabilize ABL simulations.

Realizable Dynamic LES Model

In this section, we address the realizability of a dynamic LES model with respect to two view points: first, with respect to the realizability of the underlying PDF model used to derive the dynamic LES model; and second, with respect to the realizability of the SGS stress tensor.
Our LES model (LDMK) is based on a realizable stochastic model for turbulent velocities (Heinz (2003a,b, 2007, 2008);Heinz & Gopalan (2012);Gopalan *et al.* (2013)). The model implies the exact but unclosed filtered Navier-Stokes equations. Thus, the incompressible continuity and momentum equations are given by

$$\frac{\partial \tilde{U}_i}{\partial x_i} = 0, \tag{1}$$

$$\frac{\tilde{D}\tilde{U}_i}{\tilde{D}t} = -\frac{1}{\rho}\frac{\partial \tilde{p}}{\partial x_i} + \frac{\partial(2\nu\tilde{S}_{ij})}{\partial x_j} - \frac{\partial \tau_{ij}}{\partial x_j}. \tag{2}$$

The tilde refers to space-averaged LES variables and $\tilde{D}/\tilde{D}t = \partial/\partial t + \tilde{U}_j\partial/\partial x_j$ denotes the filtered Lagrangian time derivative. In these equations, $\tilde{U}_i$ represents velocity components in i direction, $\tilde{p}$ the pressure, ρ the constant fluid density, ν the constant kinematic viscosity and finally, $\tilde{S}_{ij} = (\partial\tilde{U}_i/\partial x_j + \partial\tilde{U}_j/\partial x_i)/2$ represents the rate-of-strain tensor. The subgrid-scale (SGS) stress tensor τ_{ij} appears as an unknown on the right hand side of the momentum equation. The advantage of the underlying stochastic velocity model is that it implies in addition to the continuity Eq. 1 and conservation of momentum Eq. 2 also an equation for the SGS stress τ_{ij} (Heinz (2007)). The simplest τ_{ij} model is given by a linear stress model which implies $\tau_{ij} = \frac{2}{3}c_0 k\delta_{ij}$, where the turbulent viscosity is given by $\nu_t = k\tau_L/3$. The turbulent kinetic energy k equation reads (Heinz (2003b))

$$\frac{\tilde{D}k}{\tilde{D}t} = \frac{\partial}{\partial x_j}[(\nu+\nu_t)\frac{\partial k}{\partial x_j}] + \nu_t|\tilde{S}|^2 - \frac{2(1-c_0)k}{\tau_L}, \tag{3}$$

where $|\tilde{S}| = \sqrt{(2\tilde{S}_{ij}\tilde{S}_{ji})}$ refers to the magnitude of the rate-of-strain tensor. The time scale τ_L is defined by $\tau_L = 2(1-c_0)\Delta k^{-1/2}$. Hence, the turbulent kinetic energy equation reads

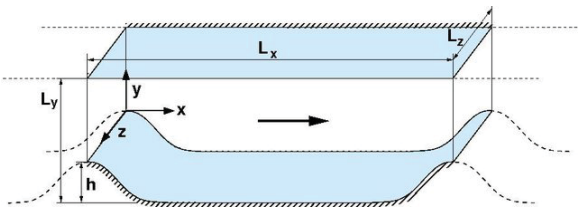

Figure 1: The two-dimensional periodic hill geometry.

$$\frac{\tilde{D}k}{\tilde{D}t} = \frac{\partial}{\partial x_j}[(\nu+\nu_t)\frac{\partial k}{\partial x_j}] + \nu_t|\tilde{S}|^2 - \frac{k^{3/2}}{\Delta}. \tag{4}$$

The closure of Eq. 4 still requires the definition of the SGS viscosity ν_t. The combination of $\nu_t = k\tau_L/3$ with $\tau_L = 2(1-c_0)\Delta k^{-1/2}$ implies the deterministic SGS model $\nu_t = 2/3(1-c_0)k^{1/2}\Delta = C_s k^{1/2}\Delta$, which will be referred to as LDM with k-equation (LDMK). Here, C_s is obtained via $C_s = L^d_{ij}M_{ji}/M_{kl}M_{lk}$. L^d_{ij} refers to the deviatoric component of the Leonard stress $L_{ij} = \overline{\tilde{U}_i\tilde{U}_j} - \overline{\tilde{U}_i}\overline{\tilde{U}_j}$ (the overbar refers to the test filter operation), and $M_{ij} = 2\Delta^T\sqrt{k^T}\overline{\tilde{S}_{ij}}$, which involves the test-filter turbulent kinetic energy $k^T = L_{nn}/2$ and filter width on the test-filter level $2\Delta = \Delta^T$.
Next, we consider the realizability condition arising from the structure of the SGS stress tensor. We have shown that τ_{ij} is a positive semi-definite matrix provided $|C_s| \leq 23\sqrt{k}/(24\sqrt{3}\Delta|\tilde{S}|)$. It should be noted that we have not assumed any specific structure of the turbulent viscosity ν_t in this derivation. Therefore, the implied turbulent viscosity bounds can easily applied in conjunction with other SGS stress models.

Results and Discussions

The objective of the present work is to analyze the demands from the stability of the realizable linear dynamic LES model (LDMK) in simulation of high Reynolds number flow. First, comparison data for the large eddy simulation are available via the channel flow DNS of Lee & Moser (2015). The primary results of channel simulations are published by the authors (Ahmadi *et al.* (2019a)) with focus on the validation against DNS data and the effect of the grid resolution. Second, to extend the study, we have considered the separated flow over a periodic hill flow studied by Mellen *et al.* (2000). Figure 1 shows the geometry of the 2D periodic hill flow. These geometries have been used for various studies and served as a benchmark for testing the performance of various turbulence models.

The size of the computational domain for channel and periodic hill simulations are $L_x = 2\pi\delta, L_y = 2\delta, L_z = \pi\delta$ and $L_x = 9h, L_y = 3.035h, L_z = 4.5h$ in the streamwise (x), wall normal (y), and spanwise (z) directions, respectively, where h is the height of the hill. The Reynold number of the flow is 37,000 based on hill height and bulk velocity above the hill crest. At the bottom and top, the channel is constrained by solid walls. No-slip and impermeability boundary conditions are used at these walls. Periodic boundary conditions are employed in the streamwise and spanwise directions. In this study simulations of the periodic hill flow are carried out on two computational grids defined in Table 1.

Table 1: Grids for simulation of periodic hill flow.

Grid	$N_x \times N_y \times N_z$	Grid size
M1	$80 \times 50 \times 30$	120 K
M2	$160 \times 100 \times 60$	960 K

To study the realizability features of the dynamic coefficient C_s involved, time series of C_s inside the channel flow at $Re_\tau = 2000$ on a resolving computational grid is monitored. Figure 2 shows the time history of C_s and its realizability bound, C_b, for two probe points along the height of the channel. Regarding the x axis it is relevant to note that time is presented by the dimensionless variable Flow-Through Times (FTT), which encounters the times flow has passed the length of the channel and calculated as:

$$FTT = \frac{t \times U_b}{L_x}. \tag{5}$$

It is conventional to call a LES simulation numerically stable when it stably runs for 100 FTT. Figure 2 presents 30 FTT of behaviour of C_s and C_b as indication of the whole time. While C_s and C_b are respectively shown in green and blue, the red circles represent the times at which C_s values hit the upper or lower realizability bounds. For the probe point close to the wall ($y^+ = 5$), in over 30 FTT (corresponding to almost 188,000 iterations), there were about 12 zones (each one consists of several iterations hitting the bounds) with C_s values hitting the lower realizability bound. With respect to the other probe point at $y^+ = 100$ (y=0.05m), the number of these events is even much higher. It means that the LDMK model applied without using realizability bounds is almost a realizable model (which is implied by its PDF-realizability), but it is not fully realizable. This can cause instability and must be treated carefully. Our recent investigations show bounding C_s from unrealizable fluctuations is the key to stabilize the unstable calculations. As previous researches show (Mokhtarpoor & Heinz (2017); Ahmadi *et al.* (2019b)), preventing C_s oscillations from unrealizable values can considerably stabilize dynamic LES in a vast range of CFL numbers. By using the SGS stress tensor realizability condition, we have made the model fully realizable and consequently numerically stable.

As mentioned before, the alternative approach to treat numerical instability is implicit LES which is stress-realizable and consequently, more stable. In addition, iLES does not require the implementation and calculation of C_s and C_b on-fly which means easier simulation setup and lower computational cost. Nevertheless, the validity of iLES depends on the validity of its basic assumption: the contribution of ν_t is small enough to be modeled by numerical dissipation. To investigate this assumption, it is very useful to observe the contribution of the kinematic turbulent viscosity for different flows. Hereby, dimensionless parameter ν^* is defined as:

$$\nu^* = \frac{\langle \nu_t \rangle}{\nu}. \tag{6}$$

to measure this contribution. Figure 3 presents ν^* obtained

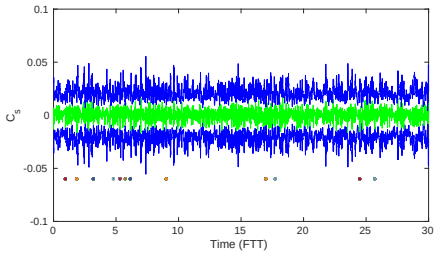

(a) $y^+ = 5$

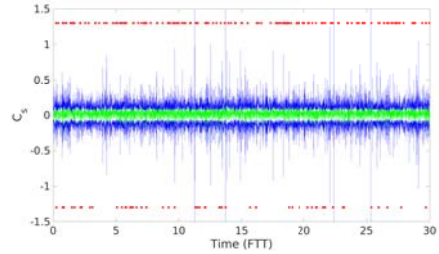

(b) $y^+ = 100$

Figure 2: Time series of SGS coefficient C_s (green) and its realizability bounds C_b (blue) in LDMK simulations of the channel flow at $Re_\tau = 2000$ for 30 FTT at two probes at different heights. The red circles indicate the times at which C_s values hit the upper and lower realizability bounds.

from turbulent channel flow LES, the most basic and fundamental case of wall bounded flow, at different Reynolds numbers and computational grids. It is important to remember that $\nu^* = 0$ in iLES. Comparison of ν^* on a computational grid fine enough to resolve flows up to $Re_\tau = 2000$ (Figure 3a), shows the contribution of the turbulent viscosity grows as a function of $Re_\tau^{1.4}$. Therefore, increasing the Reynolds number to values not accessible to DNS, e.g. as observed in ABL simulations with $Re_b \approx 10^9$, can result in considerable contribution of viscosity in form of ν_t.

At the same time, we observed how grid coarsening as well can increase the contribution of ν_t in LES calculations (Figure 3b). As expected, computational grids with high resolution and therefore, smaller LES filter width, resolve more scales of the turbulent structures and need less contribution from SGS models. Going back to the previous example of LES of ABL, we are now capable to estimate that ν^* would considerably increase in case LES involves filter width size 100 times bigger than channel flow LES.

Last but not least, ν^* can be considered to reflect the nature of the flow. Figure 4, 2D field of ν^* in the simulation of the periodic hill flow, helps us to quantify the influence from simulation of a more complex flow which includes separation and re-attachment phenomena, on the contribution of the turbulent viscosity. The Reynolds number of this flow ($Re_b = 37000$) is almost comparable to the channel flow Reynolds number at $Re_\tau = 2000$ ($Re_b = 43500$). In addition, the size of the LES filter ($\Delta = 0.028$) is almost comparable with the second coarse grid presented in Figure 3b. Nevertheless, the comparison between these two cases shows that ν^* considerably increases (grows 100 times) in the region of the separation bubble.

Each one of these parameters can make the distribution of the kinematic turbulent viscosity considerable enough to violate the validity of the iLES assumption. Figure 5 illus-

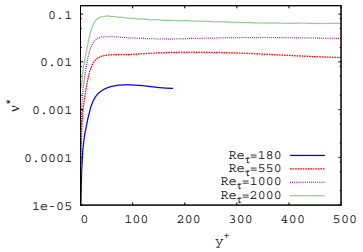

(a) $\Delta = 0.0061$

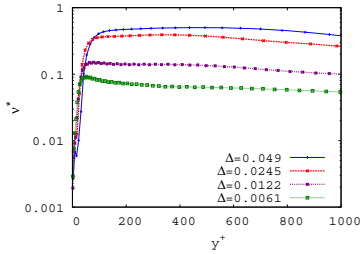

(b) $Re_\tau = 2000$

Figure 3: Turbulent viscosity contribution of wall bounded channel flow in a: different Reynolds numbers using the finest grid, b: different grid size in flow with $Re_\tau = 2000$.

Figure 4: 2D representation of ν^* in periodic hill.

trates how the combination of critical parameters can lead to wrong calculation of the flow field. Figure 5 presents the streamlines formed based on the mean velocity fields calculated by classical LES with LDMK and implicit LES at two computational grids (M1 and M2). The comparison between Figure 5a and Figure 5c reveals a noticeable deviation in the predicted characteristics of the separation bubble e.g size, shape and separation and reattachment points. Extending the study to the finer grids (Figure 5b and Figure 5d) results in more accurate simulations where the calculated separation bubble have converged to the more similar characteristics.

The shortcoming of the equation system to produce enough turbulent viscosity must be compensated by finer grids. Such a trade off does not look feasible in terms of computational costs. The computational cost implied by refining the mesh to enable the spatial grid to perform acceptable in iLES, is much more than the cost implied by on-fly calculation of C_s and C_b. In addition, refining the grid demands smaller time discretization to keep the CFL number low and

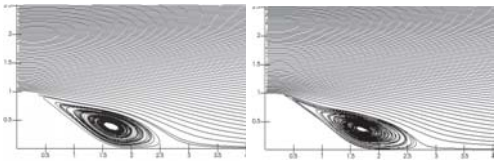

(a) LES- M1 (b) LES-M2

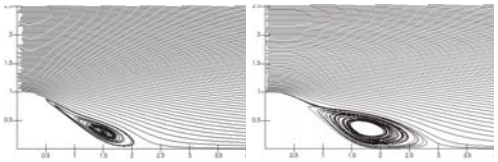

(c) iLES-M1 (d) iLES-M2

Figure 5: Stream Lines based on the mean velocity for LES and iLES at $Re_b = 37000$.

this is an extra computational cost.

At the end, the best approach to handle the numerical instability in dynamic LES without compromising the accuracy and cost, is honoring the realizability constraints imposed by the nature of the turbulent flow.

Stability of dynamic LES in ABL

Global energy demands for cheap and green energy resources motivated big wind farm projects, each one including several modern large wind turbines. To invest safe, a deep knowledge of potential power output is essential. Site assessment employs CFD simulations to investigate the local wind power within the wind farm according to the local wind speed and direction. In the context of dynamic LES, such simulations are extremely challenging while they involve simulation of kilometers of [perhaps] complex terrain resulting very coarse computational grid and perhaps separated flow. In addition, the depth of ABL (δ) is estimated to be at least around 1 km. Therefore, together with the bulk wind speed (U_b), they can build up an extremely high Reynolds number comparing to the highest Reynolds numbers studied in channel ($Re_b = 43500$) and hill flow ($Re_b = 37000$):

$$Re_b = \frac{U_b \delta}{\nu}. \tag{7}$$

Such combination of extreme conditions in ABL flow results in very unstable LES which numerically collapses very fast. The observations in this section are based on preliminary results from LES with LDMK model to simulate neutral ABL on a flat terrain taking into account Coriolis force. Simulations are performed on a computational domain $L_x \times L_y \times L_z = 3km \times 3km \times 2km$, where z is wall normal direction. The grid resolution is 10 m in x and y directions, while first cell center in the z direction is located at z=0.45 m. The final mesh consists of 13.5 M grids. It is important to notice, it is by no means possible to calculate ABL flow with a resolving computational grid which can satisfy the criteria introduced in literature for attached wall-bounded flow. The coarsest resolving grid for ABL flow can cost one a LES simulation with a mesh as big as 10^{12} cells. This is how the combination of very high Reynolds number

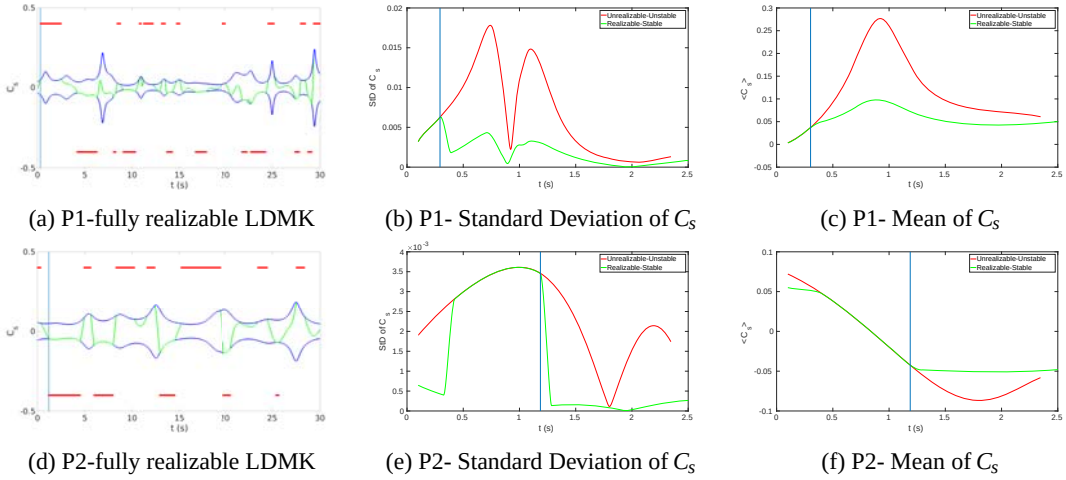

(a) P1-fully realizable LDMK (b) P1- Standard Deviation of C_s (c) P1- Mean of C_s

(d) P2-fully realizable LDMK (e) P2- Standard Deviation of C_s (f) P2- Mean of C_s

Figure 6: Time series of LES coefficient (C_s) in LES of ABL flow with $Re_b = 1.2 \times 10^9$. For detailed key description read the caption of Figure 2. The vertical blue line refers to the beginning point of the numerical instability process. Standard deviation and time-moving average values of C_s are compared between fully realizable and PDF-realizable models.

and very coarse computational grid can discredit the validity of iLES as an approach to stabilize dynamic LES.

The simulations with the fully realizable model are stable for over 100 FTT at time step $\Delta t = 0.005$ s, while it takes 171 s for the flow to pass through the domain once. In contrast, the simulation with the PDF-realizable model without stress-realizability becomes unstable after 2.35 s (0.01 FTT) at a smaller time step, $\Delta t = 0.001$ s. We tried to increase the sampling period by decreasing the time step, so the numerical instability delays and we can investigate the mechanism before the occurrence more clear. Samples are collected at 100 points and two random points at two different heights represent the others here: P1 at $z = 9.8$ m and P2 at $z = 503$ m. Figure 6 illustrates the mechanism behind the numerical instability by presenting the dynamic behavior of C_s in time. Let us first look at Figure 6a and observe the dynamic behavior of C_s and its stress-realizable bounds in 30 s. After a short time (0.2935 s, marked by vertical blue line), C_s hits the upper realizable dynamic bound C_b for the first time. This means here for the first time, the calculation of C_s tends to a value which violates the realizability of the stress tensor. At the exact same moment, the standard deviation of fully realizable and only PDF-realizable models deviate from each other drastically (see Figure 6b). The unrealizable status seems to be damped in the fully realizable model resulting in a stable LES. Where the sudden increase of the standard deviation in the absence of stress-realizable bounds, builds up to a numerical instability which stops the simulation after 2.35 s. The sudden relative increase of the standard deviation of C_s in the model with no bounds, also influence C_s moving average as presented in Figure 6c. It is important to notice that the behavior shown in this figure belongs to a random point and every point experiences a different time history regarding C_s calculations. As another sample point in the domain, history of C_s and C_b at P2 are presented in Figure 6d. At P2, the event leading to the numerical instability starts at $t = 1.18$ s by hitting the lower bound for the first time. The same pattern suddenly appears in the behavior of the standard deviation of C_s. In a split of second, unrealizable coefficient adopt values 20 times larger than the realizable model. This behavior is found to be repetitive among all the points. As a result of piling up such unrealizable high standard deviation, the equation system behind the simulations tend to numerical instability. Although the PDF-realizable dynamic of the equations tries to stabilize the simulation, this can not be done without the company of the stress-realizable constraints.

Conclusions

The main goal of this paper is to investigate the demands of numerical stability of dynamic LES of a wall-bounded flow at a very high Reynolds number. To show this, the preliminary results from the simulation of neutral ABL flow on a flat terrain is presented at $Re_b = 1.2 \times 10^9$ as a test case. The simulations were found to be extremely unstable without a suitable stabilizing technique. It is estimated to be even more challenging to extend the simulations to the complex terrain simulations including separation and re-attachment of the flow and taking into account thermal gradients due to the sun radiation. A PDF-realizable LES model was found to be not fully stress-realizable, which can cause numerical instabilities. We have derived a condition for the realizability of the SGS stress tensor, which made the non-equilibrium (LDM) fully realizable. Stability analyses performed for a high Reynolds number separated flow demonstrated that the new fully realizable LES model (LDMK) is always stable for a wide range of CFL numbers. This approach is easily applicable to stabilize other dynamic LES models. While alternative stabilization concepts (constant clipping or averaging in space), in comparison, suffer from limiting assumptions and professional manual model setup. We also presented realizable dynamic LES applied to other flows, like turbulent channel flows covering a range of Reynolds numbers. Comparisons with implicit LES without SGS model, which are often applied to test numerical schemes, are interesting because such models are stress-realizable but not PDF-realizable. Consequently, iLES does not suffer from numerical instability but comes with shortcomings of its own. Its equation system by nature is unable to produce kinematic turbulent viscosity and this can result in inaccurate results in some conditions. For increasing Reynolds number, remarkable differences are found between iLES and fully realizable methods. Evaluating the

results on the computational grids with different mesh resolutions magnifies the lack of validity of iLES. Not being PDF-realizable makes iLES very sensitive to the size of filter width. In order to compensate a SGS model, iLES demands very high grid resolution leading to very expensive, almost non-affordable, computations. The overall conclusion of these studies is that methods honoring all relevant realizability principles offer significant advantages compared to methods that do not honor realizability constraints.

Acknowledgement

This paper is published as part of PhD research financed by Hans Böckler Stiftung and in assistance with many colleagues.

The simulations were performed at the HPC Cluster EDDY, located at the University of Oldenburg (Germany) and funded by the Federal Ministry for Economic Affairs and Energy (Bundesministeriums fr Wirtschaft und Energie) under grant number 0324005.

REFERENCES

Ahmadi, G., Peinke, J., Kassem, H., Stoevesandt, B. & Heinz, S. 2019a Wall-bounded turbulent flows up to high reynolds numbers: Les resolution assessment. In *AIAA SciTech 2019*, pp. 19–1887.

Ahmadi, G., Peinke, J., Kassem, H., Stoevesandt, B., Mokhtarpour, R. & Heinz, S. 2019b Realizable dynamic les of high reynolds number turbulent wall bounded flows. In *AIAA SciTech 2019*, pp. 19–2140.

Aspden, A., Nikiforakis, Nikos, Dalziel, Stuart & Bell, John 2008 Analysis of implicit les methods. *Communications in Applied Mathematics and Computational Science* **3**, 103–126.

Deskos, Georgios, Laizet, Sylvain & Piggott, Matthew 2018 Turbulence-resolving simulations of wind turbine wakes. *arXiv preprint arXiv:1804.07508* .

Drikakis, D., Kwak, D. & Kiris, C.C. 2016 Computational aerodynamics: advances and challenges. *Aeronautical Journal* **120**, 13–36.

Germano, M. 2000 Fundamentals of large eddy simulation. In *Advanced Turbulent Flows Computations* (ed. R. Peyret & E. Krause), *CISM Courses and Lectures*, vol. 395, pp. 81–130. Berlin, Heidelberg, New York: Springer.

Germano, M., Piomelli, U., Moin, P. & Cabot, W. 1991 A dynamic subgrid-scale eddy viscosity model. *Physics of Fluids* **3** (7), 1760–1765.

Ghosal, S., Lund, T. S., Moin, P. & Akselvoll, K. 1995 A dynamic localization model for large-eddy simulation of turbulent flows **286**, 229–255.

Gopalan, H., Heinz, S. & Stöllinger, M. 2013 A unified ransles model: Computational development, accuracy and cost. *Journal of Computational Physics* **249**, 249–274.

Heinz, S. 2003a *Statistical Mechanics of Turbulent Flows*. Springer-Verlag, Berlin, Heidelberg, New York, Tokyo.

Heinz, S. 2003b On fokkerplanck equations for turbulent reacting flows. ii. filter density function for large eddy simulation. *Flow, Turbulence and Combustion* **70**, 153–181.

Heinz, S. 2007 Unified turbulence models for les and rans, fdf and pdf simulations. *Theoretical and Computational Fluid Dynamics* **21** (2), 99–118.

Heinz, S. 2008 Realizability of dynamic subgrid-scale stress models via stochastic analysis. *Monte Carlo Methods and Applications* **14**, 311–329.

Heinz, S. & Gopalan, H. 2012 Realizable versus non-realizable dynamic subgrid-scale stress models. *Physics of Fluids* **24**, 1–23.

Lee, Myoungkyu & Moser, Robert D. 2015 Direct numerical simulation of turbulent channel flow up to $re_\tau = 5200$. *Journal of Fluid Mechanics* **774**, 395–415.

Lilly, D. K. 1992 A proposed modification of the germano subgrid-scale closure method **4** (3), 633–635.

Lund, T., Ghosal, S. & P.Moin 1993 Numerical experiments with highly variable eddy viscosity model. In *Engineering Applications of Large Eddy Simulations* (ed. S. A. Ragale & U. Piomelli), *CISM Courses and Lectures*, vol. 162, pp. 07–11. ASME.

Mellen, C.P., Fröhlich, J. & Rodi, W. 2000 Large-eddy simulation of the flow over periodic hills. In *Proceedings of 16th IMACS world congress*, pp. 1–6.

Meneveau, Charles & Katz, Joseph 2000 Scale-invariance and turbulence models for large-eddy simulation. *Annual Review of Fluid Mechanics* **32**, 1–32.

Meneveau, C., Lund, T.S. & Cabot, W. 1996 A lagrangian dynamic subgrid-scale model for turbulence **319**, 353–385.

Mokhtarpoor, Reza & Heinz, Stefan 2017 Dynamic large eddy simulation: Stability via realizability. *Physics of Fluids* **29** (10), 105104.

Piomelli, U. 1999 Large-eddy simulation: achievements and challenges. *Physics of Fluids* **35** (4), 335–362.

Piomelli, U. & Liu, J. 1995 Large-eddy simulation of rotating channel flows using a localized dynamic model **7**, 839–848.

Pope, S. B. 2000 *Turbulent flows*. Cambridge University Press, Cambridge.

Ritos, K., Kokkinakis, I.W. & Drikakis, D. 2017 Physical insight into the accuracy of finely-resolved iles in turbulent boundary layers **169**, 1–8.

Sagaut, P. 2002 *Large eddy simulation for incompressible flows: an introduction*. Springer-Verlag, Berlin, Heidelberg, New York, Tokyo.

Spalart, P. R., Jou, W. H., Strelets, M. & Allmaras, S. R. 1997 Comments on the feasibility of les for wings, and on a hybrid rans/les approach. pp. 4–8. Columbus, Ruston, LA, USA: Greyden Press.